Hydrol. Earth Syst. Sci. Discuss., 7, 3551–3589, 2010
www.hydrol-earth-syst-sci-discuss.net/7/3551/2010/
doi:10.5194/hessd-7-3551-2010

Hydrology and Earth System Sciences Discussions

WRF simulation of a precipitation event over the Tibetan Plateau, China – an assessment using remote sensing and ground observations

F. Maussion[1], **D. Scherer**[1], **R. Finkelnburg**[1], **J. Richters**[1], **W. Yang**[2], **and T. Yao**[2]

[1]Institut für Ökologie, Technische Universität Berlin, 12165 Berlin, Germany
[2]Institute of Tibetan Plateau Research, Chinese Academy of Sciences (CAS), Beijing 100085, China

Received: 30 May 2010 – Accepted: 8 June 2010 – Published: 16 June 2010

Correspondence to: F. Maussion (fabien.maussion@tu-berlin.de)

Published by Copernicus Publications on behalf of the European Geosciences Union.

Abstract

Meteorological observations over the Tibetan Plateau are scarce, and precipitation estimations over this remote region are difficult. Numerical weather prediction models can be used to retrieve precipitation fields at a higher spatial and temporal resolution than the commonly used gridded precipitation products. In this paper, the Weather Research and Forecasting (WRF) model capacity in retrieving rain- and snowfall during a single event is evaluated. The simulated event is the tropical cyclone RASHMI (22–28 October 2008). The simulations are conducted with three nested domains, with a mesh size of 30, 10, and 2 km. The output of the model in each resolution is compared to the Tropical Rainfall Measuring Mission (TRMM) dataset for precipitation and to the Moderate Resolution Imaging Spectroradiometer (MODIS) dataset for snow. TRMM and WRF precipitation products are then compared to ground based measurements: both datasets agree on the spatial repartition of precipitation, but differ on the retrieval of strong precipitation events. The results suggest an overall improvement from WRF over TRMM with respect to ground based measurements. In a second part, various physical parameterizations schemes of the model are compared. Their impact on WRF precipitation output is small, this suggests that model errors during the event may have other causes.

1 Introduction

The Tibetan Plateau (TiP) is the source of many major rivers in central Asia, affecting the livelihood of hundreds of millions of people in the surrounding regions. Its glaciers are characteristic elements of the natural environment, forming water resources of cardinal importance for both ecosystems and local population. Several studies have shown the determining impact of the Plateau orography and boundary layer on the monsoon system (Gao et al., 1981; Hahn and Manabe, 1975). More particularly, the influence of spring snow cover on monsoon onset and intensity was investigated e.g.

HESSD

7, 3551–3589, 2010

by Wu and Qian (2003), who noted the correlation of spring snow cover anomalies with the repartition and intensity of summer precipitation over central Asia. Focusing on the monsoon history over the past, present and future, the Sino-German Priority Programme 1372 (Appel and Mosbrugger, 2006) was initiated by the Deutsche Forschung Gemeinschaft (DFG) to develop a multidisciplinary approach dealing with the complex processes and interactions taking place between the major driving forces on the Plateau.

Kehrwald et al. (2008) and Yao et al. (2007) underlined the importance of the Tibetan and Himalayan glaciers on the hydrological features in Asia, and noted the threat of climate change over the "Third Pole"; Kang et al. (2009) emphasized the peculiar sensitivity of cold-based glaciers in central Tibet to precipitation seasonality and intensity. Located in a transition zone under the complex influence of both the continental climate of central Asia and the Indian Monsoon, the Nam Co basin and its water supplying neighbour the Nyainqentanglha range have been pointed out as a key research area in Tibet. The recent Nam Co lake level rising has been attributed to glacial melt as well as to an increase of precipitation in recent decades (Wu and Zhu, 2008). Precipitation increase in central TiP during this period has also been documented by Liu et al. (2009).

The TiP remains a sparsely observed region, and the meteorological data available to the scientific community lacks of spatial dispersion as well as long term records necessary for reliable climatological studies (Frauenfeld et al., 2005). More than any other parameter, precipitation data suffers from strong terrain dependence and can hardly be acquired by the usual gridded precipitation products, especially over the Plateau (Ma et al., 2009; Yin et al., 2008). The constantly improving capabilities of the numerical weather prediction models can be used to retrieve this lack of information, by providing precipitation fields and other relevant meteorological variables at high resolutions. The usage of weather models in challenging configurations is widely evaluated and documented for some regions of the world (e.g., Caldwell et al., 2009 for the Californian mountains, Box et al., 2006 over Greenland).

HESSD
7, 3551–3589, 2010

However, the capacity of the models in retrieving snowpack and precipitation amounts in complex terrain is still discussed. Using higher horizontal spatial resolutions (less than 10 km) has been advanced as a substantial improvement, as they allow a more accurate representation of the mountainous terrain. Nevertheless, the physics of convective systems is still too imprecise to resolve completely the small scale processes taking place in mountainous regions, and increasing spatial resolution will have a much more positive impact by using adapted boundary input data (Mass et al., 2002). The effect often cited as orographic bias is described as an over-prediction of precipitation in mountainous regions while predicted snowfall amounts often lie under measured values (e.g., Leung and Qian, 2003). This bias can be attributed to model physics as well as to an improper representation of the small scales and vertical moisture transfers.

1.1 Objectives

In this paper, the capacity of the Weather Research and Forecasting (WRF) model in retrieving snow and liquid precipitation amounts during a single precipitation event is evaluated. To our knowledge, only few studies assessed or made use of the WRF model on the TiP area. Li et al. (2009) investigated the impact of Nam Co lake surface skin temperature additional input on a short-range precipitation event simulation. Zhu and Chen (2003) simulated a convective system and observed the sensitivity of the non-hydrostatic Mesoscale Model (MM5) to the low-level thermal forcing and the land-coverage over the TiP, while Sato et al. (2008) analysed accurately the sensitivity of precipitation diurnal cycle to the horizontal grid spacing. Their results show that the finest resolutions (7 km) are more efficient in representing diurnal clouds formation and activity than coarser grids. Tang et al. (2007) and Gao et al. (2006) explored the role of the TiP topography on the simulation of precipitation in China, but stayed geographically on the edges of the Plateau and did not observe precipitation on the TiP itself. Peng et al. (2009), finally, observed the positive feedback of the assimilation of ground based observations on the slope of the TiP for quantitative precipitation forecasts over

HESSD
7, 3551–3589, 2010

China. In this study, three main questions are addressed:

1. What are the validation tools and data available to the community to assess the performance of the model, and are they consistent enough for this purpose?

2. Is it possible, between the numerous physical and spatial configurations of the WRF model, to propose a set-up that would be more adapted to the TiP area?

3. Is the model able to simulate and retrieve realistic precipitation fields in this mountainous and sparsely observed region?

These questions are generally treated separately. To assess the performance of a model when running sensitivity studies, for example, observations will often be taken as an absolute reference, which allows the decision process inherent to the second question (Rakesh et al., 2007; Yang and Tung, 2003). The first two questions have been formulated with the intention of realizing a meaningful inter-comparison of precipitation products and forecast assessment tools, taking the reasonable risk of losing clarity. To avoid this, the spatial and temporal frame of the study will be defined precisely. Only after having answered the first question and analysed the impact of increasing resolution on precipitation estimations, at least partially, we will present the results of a sensitivity study run on five different physical parameterizations of the WRF model.

1.2 Study area

We will focus on the output of WRF over the central and south-eastern TiP, and more precisely on the Nam Co basin and the Nyainqentanglha Mountains (NyM). This region, starting from the the Nam Co Lake on its western side and extended to the very south-east of the Tibetan Autonomous Region, contains many glaciated areas. The western part near Nam Co, dry and cold, includes the major high peaks (up to 7000 m a.s.l.) and holds mostly continental (subpolar) polythermal glaciers while the eastern part, much

HESSD
7, 3551–3589, 2010

more under summer monsoon influence and averaging at a lower altitude, holds sensitive temperate maritime glaciers (Shi and Liu, 2000). Due to its vicinity to the ocean and the lower plains of India and Bangladesh, one observes here a strong climatic seasonality and intense summer precipitation.

1.3 Event description

The complex terrain on the edges of the TiP and its blocking effect on moisture transfer coming from the Indian and Pacific Oceans has a characteristic impact on the formation of orographic induced storms (Chen et al., 2007), causing strong and violent precipitation events counting for a substantial part of the yearly precipitation records. The tropical cyclone RASHMI formed in the Bay of Bengal on 24 October 2008 and reached the coast on 27 October. Strong winds and heavy rainfalls occurred over Bangladesh and India, causing substantial damages and taking people lives (the India Meteorological Department made a comprehensive description of the event in IMD, 2008). The system weakened rapidly after reaching lands, carrying along further precipitation in the form of snow on the Himalayas and the TiP. This event happened after the monsoon period and is challenging the model by its complexity: cyclonal formation overseas and snowfall event over the TiP.

2 Data and methods

2.1 Model and experiment design

The mesoscale model used in this study is the community WRF-ARW model, version 3.1.1, developed primarily at the National Center for Atmospheric Research (NCAR) in collaboration with different agencies like the National Oceanic and Atmospheric Administration (NOAA), the National Center for Environmental Prediction (NCEP), and many others. The WRF is a limited area, non hydrostatic primitive

HESSD
7, 3551–3589, 2010

equation model with multiple options for various physical parameterization schemes (Skamarock et al., 2008). The experimental set-up is resumed in Table 1.

Motivations for this physical parameterization set-up can be found in Chin (2008), for another geographical region though. The simulation covers the period 22–28 October 2008, totalizing seven 36 h long runs starting at 12:00 UTC, each run contributing to 24 h effective output (all dates and times are in Universal Time Coordinate). Meteorological input datasets are the standard final analysis (FNL from GFS) data with additional sea surface temperature (SST) input. The two-way nesting capabilities of the WRF are used to rescale the domains on the study area (Fig. 1): the 10 km domain covers a large part of the TiP and the whole NyM in its central part, and the 2 km finest domain is centred on the Nam Co basin. This region contains many lakes (the most import one being the Nam Co lake with an area of 1980 km^2) that have a significant impact on the local climate and atmospheric moisture content (Haginoya et al., 2009). The current pre-processing chain from WRF does not handle properly the lake temperatures and sets the water temperature either to an arbitrary value or, when a SST field is available, to the SST value. In our case, this leads to dramatic errors as the standard product we used is only available for seas and oceans: the temperature is simply extrapolated from the Bay of Bengal without considering elevation. As proposed by Li et al. (2009), we used remote sensed skin temperatures to retrieve the lake temperature. We used the Moderate Resolution Imaging Spectroradiometer (MODIS) 8-day land surface temperature product version 5 (MODA11 8-DAY 1KM L3 LST, 23–30 October 2008). The mean temperature of all water covered grid cells was computed for the day and the night time scenes, to obtain a mean surface temperature of 4.9 °C. This value is consistent with the climatology of Haginoya et al. (2009) and was used to initialize the model water temperature each day and for each resolution over Nam Co and surrounding water bodies. This corrected the initial error thoroughly and the omissions that are made doing these approximations are considered as negligable for this event. The concrete impact of lake temperature initialization will be analysed more accurately in a future study.

HESSD
7, 3551–3589, 2010

2.2 Evaluation datasets

2.2.1 TRMM precipitation

The WRF model output is compared to the precipitation data of the Tropical Rainfall Measuring Mission (TRMM). The mission provides precipitation estimates at fine spatial scales using a calibration based sequential scheme and data from multiple satellites as well as rain gauge analysis. In this study the 3B42 version 6 product is used (Huffman et al., 2007). This is a product spanning a global belt from from 50° N to 50° S with a spatial resolution of 0.25°, with outputs at 3 h interval. The four steps algorithm estimates precipitation with a combination of passive microwaves sensors calibrated with infrared (IR) estimates to provide the best adjustment at each grid box, and finally rescales the 3 hourly product to the monthly dataset, indirectly using rain gauge data to perform a bias correction. The 3 hourly series are then concatenated to 24 h precipitation amounts.

2.2.2 MODIS snow cover

Moderate Resolution Imaging Spectroradiometer (MODIS) refers to two instruments currently collecting data as part of NASA's Earth Observing System (EOS) program. The MODIS/Terra Snow Cover Daily L3 Global 500 m Grid (MOD10A1) contains snow cover, snow albedo, fractional snow cover, and Quality Assessment (QA) data in compressed Hierarchical Data Format-Earth Observing System (HDF-EOS) format along with corresponding metadata. A single MOD10A1 dataset consists of 1200 km by 1200 km tiles of 500 m resolution data gridded in a sinusoidal map projection. MODIS snow cover data are based on a snow mapping algorithm that employs a Normalized Difference Snow Index (NDSI) and other criteria tests (Hall et al., 2006). Within the pre-processing of the MODIS datasets, valid and data of high quality, based on the QA assessment, were selected for the evaluation of WRF modelling runs.

HESSD
7, 3551–3589, 2010

2.2.3 Ground meteorological stations

The data used in this study is the Global Summary of the Day from the National Climatic Data Center (NCDC; http://www.ncdc.noaa.gov/oa/ncdc.html). Various daily summary elements such as temperature (mean, max, min), dew point, wind speed (mean, max, peak gust), pressure, visibility, precipitation, snow depth (depending on how well the station is equipped) can be downloaded free of charge. All the stations should respect the recommendations of the World Meteorological Association (WMO) and the data passes quality control before being published. We focus on the output from WRF over the TiP. Therefore the stations selected for this study follow two criteria: they must be located within the area covered by the second nested domain and be situated above 3000 m a.s.l. A number of 19 stations is available for this period, showing how the TiP still lacks of observations. Moreover, they are not homogeneously distributed over the test area and are indeed concentrated in the more densely populated areas in the south-eastern part of the plateau (Fig. 1). In addition, precipitation data measured at the Nam Co Monitoring and Research Station operated by the Institute of Tibetan Plateau Research, Chinese Academy of Sciences (ITP-CAS) was used to assess the WRF Model precipitation output on the Nam Co lake region (30°46′ N, 90°59′ E, 4730 m a.s.l, located in the south east shore of the lake).

2.3 Statistical evaluation parameters

A few parameters broadly used in the community are defined to statically assess the performance of the model. Some of them are derived from a contingency table (Wilks, 1995). This table represents a 2×2 matrix (Table 2), where each element of the matrix holds the number of occurrences of a certain event, which has been detected by observation and/or by the model in a given statistical population (gridded dataset, observation days, ...). Based on this table, many possible scores can be defined and be found in the literature. In this study, five indicators are used.

HESSD
7, 3551–3589, 2010

The bias score (BIAS) is defined as:

$$\mathrm{BIAS} = \frac{F}{O} = \frac{A+B}{A+C} \tag{1}$$

where F is the number of points where the event was forecasted, and O is the number of points where the event was observed. This score is an indicator of how well the model recovered the number of occurrences of an event, regardless to its spatio-temporal repartition. In addition to the BIAS, the False Alarm Rate (FAR) computes the portion of the predicted events that where actually "non-events":

$$\mathrm{FAR} = \frac{B}{F} = \frac{B}{A+B} \tag{2}$$

The Probability Of False Detection (POFD), gives an information on the portion of wrongly predicted events in the total "no" observations:

$$\mathrm{POFD} = \frac{B}{\mathrm{NO}} = \frac{B}{B+D} \tag{3}$$

where B is the number of forecasted occurrences that where not observed and NO is the total of observed "non-events". As well as the FAR, it is not a perfect indicator as it depends on the number of "no" occurrences, but is convenient to realize forecast inter-comparisons, as it does not depend on the number of "no" predictions from the model itself. The same principle can be used to define the Probability Of Detection (POD) that, in parallel to the POFD, proposes a simple way to assess a forecast by giving the portion of correct forecast over all the "yes" events:

$$\mathrm{POD} = \frac{A}{\mathrm{YES}} = \frac{A}{A+C} \tag{4}$$

Finally, to concretely evaluate the simulation efficacity, the Heidke Skill Score (HSS) is defined:

$$\mathrm{HSS} = \frac{A - A_{\mathrm{Ref}}}{A_{\mathrm{Perf}} - A_{\mathrm{Ref}}} \tag{5}$$

HESSD
7, 3551–3589, 2010

where A is the forecast score, A_{Ref} the probability of detection by chance and A_{Perf} the score obtained by a perfect forecast:

$$A_{\mathrm{Ref}} = \frac{(A+B)(A+C)+(B+D)(C+D)}{N^2} \tag{5a}$$

$$A = \frac{H}{N} = \frac{A+D}{N} \tag{5b}$$

$$A_{\mathrm{Perf}} = 1 \tag{5c}$$

H is the number of correctly forecasted events ("hits") and N is the size of the considered population. The HSS evaluates the ability of a forecast to be better or worse than a random forecast, and ranges from −1 to 1 (1 for a perfect and 0 for a random forecast). In addition the contingency table based scores, the standard Mean Bias (MB) and Root Mean Square Deviation (RMSD) parameters are defined as:

$$\mathrm{MB} = \frac{1}{N}\sum_{n-1}^{N}(P_{\mathrm{m}} - P_{\mathrm{o}})_n \tag{6}$$

$$\mathrm{RMSD} = \sqrt{\frac{1}{N}\sum_{n-1}^{N}(P_{\mathrm{m}} - P_{\mathrm{o}})_n^2} \tag{7}$$

where P_{m} and P_{o} are modeled and observed precipitation on a grid point.

3 Results

The WRF simulation covers three different areas in increasing resolution (Fig. 1): the large domain that covers central Asia, the medium domain that contains a large part of the TiP, and the small domain that is centred on the Nam Co Basin. To avoid conflicting definitions between geographical domains and model resolutions, WRF output

HESSD
7, 3551–3589, 2010

in the three resolutions (30 km, 10 km and 2 km) will be named WRF30, WRF10 and WRF2. In the presentation of the results, the different outputs will also be analysed in increasing resolution: contingency table based evaluation methods will be applied to WRF30 in comparison with TRMM (0.25° resolution), and then to the snowfall output of WRF10 and WRF2 in reference to MODIS (500 m resolution). After this, the impact of rescaling on the operational output will be assessed by comparing all available data to ground based measurements. Finally, the convenient evaluation methods will be applied to different experiments to assess the model sensitivity to various physical parameterizations.

3.1 Precipitation observed by TRMM

3.1.1 Synoptical study

In the first place, the mesoscale situation is visually analysed: WRF30 and TRMM daily precipitation fields during the cyclone life are presented in Fig. 2, where the rough cyclonal patterns can be observed and recognized. The track of the cyclone is easily traceable and the precipitation amounts following its movement are considerable according to both TRMM and WRF, but one can establish considerable discrepancies. On the 24 and 25 October 2008, the maximum of precipitation amount seen by TRMM is clearly following the cyclone eye, but in the WRF output the same eye is recognizable by the absence of precipitation (in spite of its movement during the 24 h). The same pattern is to observe on the 26, when the cyclone reaches the coast. The areas affected by precipitation are mostly the same in both datasets, but one can observe a certain spatial shift in precipitation maximums (on the 26, the maximum is overseas for TRMM whereas WRF already predicts most precipitation over Bangladesh). This disparity, however, diminishes when the cyclone reaches land, and will therefore not be studied further down. On the Himalayas and the TiP, the patterns comparison is more satisfying. The two maximums induced by the blocking effect of the Himalayas over the slopes of Bhutan and the eastern NyM on the 27 October are observable on

HESSD
7, 3551–3589, 2010

both datasets, as well as the extending precipitation front over the plateau. However, recovered amounts and surfaces are generally larger in WRF30 than in TRMM.

3.1.2 Statistical scores

The 0.25° grid of the TRMM dataset is fitted to WRF30 using nearest neighbourhood to facilitate pixel-based comparison. The purpose here is not only to describe the difference of the model with TRMM, but to underline the translation of visual interpretations in contingency table based scores when comparing two gridded data-sets. During the cyclone life, much precipitation occurred over oceans and shall not enter in the frame of this study. Therefore, the two grids have been cropped to cover the same area as the medium domain, totalizing a number of 50 × 50 grid points covering a large part of the TiP. Using the contingency tables defined in Sect. 2.3, three thresholds (10, 50 and 100 mm) where applied to the seven days accumulated precipitation fields (22–28 October 2008); a similar method was already applied by Rakesh et al. (2007). Results are presented in Fig. 3. The two datasets are in good concordance for the smaller precipitation amounts and show a growing discrepancy for higher thresholds. The 10 mm precipitation fields extend more to the west in TRMM and to the north in WRF30 but the scores attest a good overall concordance. The precipitation maximum (more than 100 mm) on Eastern NyM (NE India) has been tracked by both TRMM and WRF, but the model predicted much more events over the Himalayas. The considered scores follow this visual interpretation. More than 90% of WRF forecasted 100 mm events were not observed by TRMM. However, only very few grid points were found positive by TRMM and not by WRF (constant POD of about 0.85 for the three thresholds). The Heidke Skill Score (HSS), finally, resumes fairly well the good concordance of model and TRMM for lower thresholds, and their comparatively small correlation for higher amounts (a random forecast would have a HSS of zero). Considering the 2500 grid points, WRF RMSD and MB are respectively 63 and 27 mm, statistics that give only limited information.

HESSD
7, 3551–3589, 2010

3.2 Snowfall observed by MODIS

In WRF output, most of the precipitation over the TiP fell as snow. To verify the model prediction, we selected two MODIS scenes with a relatively sparse cloud coverage, on 22 and 29 October 2008 (before and after the simulated period). The scenes were taken around 05H UTC each day, and the accumulated snowfall amounts from WRF on the period 22–28 October were computed for comparison. The MODIS scenes depicted the large snow cover area changes in the southeastern TiP within this short period, which allows us to apply categorical scores to WRF10 and WRF2.

The domains edges are cropped of five pixels on each side of the grid to discard numerical boundaries effects and the MODIS scenes are filtered as follows: pixels obscured by clouds in one of the scenes and pixels covered by water are removed from the statistical population, as well as the cells containing snow in both scenes where no event can be detected. From 19600 cells before filtering, a total of 9359 and 8776 cells for respectively the medium and the small domains where available to determine the occurrence of the snowfall event. The percentage of grid points where snowfall was detected is respectively 22% and 84%. The problem now is to define how a grid cell in the WRF output can be classified as snow event or not. A first statistical evaluation was made to determine the threshold to apply to the simulated snow amounts. The HSS score in relationship to the threshold is showed on Fig. 4. The same exercise can be done on WRF10 output over the small domain, but the available population is smaller (900 cells from which 365 are available for the test). This should not affect the relevance of the scores and the results are therefore comparable to WRF2 over the same geographical region.

The best score is reached on WRF10, when applying a threshold of 7 mm to the accumulated snow amounts. This threshold seems physically reasonable, considering the probable melt during the simulation time and the amount of snow necessary to cover the ground sufficiently to be detected by MODIS. The same method applied on the smaller domain, for a comparable grid point population, provided lower scores.

HESSD
7, 3551–3589, 2010

On such a case, when the yes event is predominant, the categorical statistics indeed assess the capacity of the model to retrieve the non events, because the number of hits by chance becomes very high and the statistical success definition more confuse. The maximum is reached at 2 mm, which is too low and underlines the smaller performance of the model on this domain. The thresholds of 2 and 7 mm were applied to the grid to analysis (Fig. 5).

The geographical repartition of snowfall is close to MODIS on the large scale: the snow/rain limit in Northern Bhutan and India is spotted rigorously, and the snow areas correspond in most regions. The snow limit is a bit further north in MODIS, and some isolated grid points on the northeastern TiP were not caught by WRF. This suggests that the limit of precipitation is also further north than detected by TRMM (Fig. 3). However, the model did not catch properly the extension of snow on the western part of Nam Co, where both TRMM and MODIS detected precipitation. The threshold of 2 mm is definitively too low when applied on the medium domain. The threshold of 7 mm on the smaller domain corresponds to a smaller score: simulated precipitation fields did not reach the eastern regions where snow changes were observed. We cannot observe any significant difference between WRF10 and WRF2 over the Nam Co Basin, as the errors concern the same areas (not shown).

3.3 Meteorological observations

In the two upper paragraphs, WRF precipitation output for each grid cell was classified in arbitrary categories (light rain, heavy rain or snow events). If the contingency scores give an indication of how well the model roughly performed, they say relatively few about the error itself, and about the geographical repartition of this error (unless plots like Figs. 3 or 5 are presented, which is not always the case when using skill scores). If one employs the term “model performances”, it also implies that the observational gridded dataset is taken as absolute reference (per definition, Table 2). This statement shall always be put into question.

HESSD
7, 3551–3589, 2010

As first approach, the cumulated rainfall on the seven observation days is analyzed station per station. The output from the nearest grid cell of the four datasets (TRMM, WRF30, WRF10 and WRF2) is compared to measured values (Table 3). The accumulated precipitation time series of nine selected stations are plotted on Fig. 6. We will refer to the stations with their names but the reader should refer to their identification number to make links with TRMM and MODIS observations.

The results illustrate the overall discrepancy that was to expect on a short event: some stations show consistent values for all datasets, but in some cases the differences are dramatic. The stations Lhunze (6), Tingri (14), Sog Xian (13) an Xainza (16) are located in "C-zones" (Fig. 3), where TRMM predicted 10 and 50 mm events while WRF did not. In the four cases, WRF was actually closer to the records while TRMM over predicted the amounts. On Sog Xian and Lhunze time-series, all three datasets agree on rainfall timing, but TRMM over-estimated the amounts. At Pagri (10), strong precipitation was also recorded but WRF under-estimated the amounts. The other way around, the stations Deqen (4) and Yushu (18) are located in "B-zones", where WRF forecasted an event that was not spotted by TRMM. The time series confirm that in these examples, WRF retrieved satisfyingly both amounts and arrival time of the precipitation front (with one day shift at Deqen, however). Deqen and Yushu are located on the western part of the front and both station records suggest (but do no demonstrate) that the actual precipitation patterns may extend further in the western TiP than proposed by TRMM. If often the amounts do not match, the time-series show a general good concordance of TRMM and WRF on the timing, with reasonable shifts of a few hours. Nevertheless, WRF over estimated precipitation amounts e.g. at the stations Dege (2), Nyingchi (9), Qamdo (11), Zadoi (19) and Nam Co (20). For several stations (e.g., Baingoin, Pagri) the three dataset closely agree, whereas some stations do not allow a clear statement on which dataset is closer to reality. Lhasa, for example, is located in a precipitation area for both TRMM and WRF, but recorded only a few millimeters of snow. The ground based measurements can also be put into question and may not always be representative of the surrounding precipitation features.

HESSD
7, 3551–3589, 2010

The first conclusions enunciated looking at each station separately are also evident in the summary statistics (RMSD and MB). For this event, WRF seems to be closer to observations than TRMM, but has a tendency to overestimate precipitation amounts. This positive bias in TRMM and WRF may be explained by the nature of precipitation that mostly came in the form of snow. The RMSD and MB scores have also the disadvantage to be strongly influenced by bigger amounts: they often reflect the extreme discrepancies whereas the comparatively bad forecasts for smaller events are almost not considered (if we remove the station Deqen from the evaluation, the RMSD are then 20.4, 17.04, 13.82 mm for TRMM, WRF30 and WRF10).

The improvement brought by the 10 km resolution is clearly noticeable. Unfortunately, no further evaluation for WRF2 could be made because only four stations are available in this small area. For these stations, the difference with WRF10 suggested a small but overall improvement. The use of the two-way nesting option to run the model, by adding the feedback from the inner nested domain to the parent grid at each integration step shall generally improve the forecast of the parent and child domain, and creates consistent fields for all domains (Fig. 7). In this illustration, WRF2 seems to produce more realistic features but this is not verifiable in the statistics.

3.4 Influence of model physics

In Sects. 3.1 to 3.3, we compared the output of the model with three reference datasets. In this part, the sensitivity of the model to different physical parameterizations schemes (PPSs) will be evaluated. The purpose is to evaluate if the PPSs, among other error factors, have a dominant impact on the precipitation output. The divergences between the control experiment (CO1) and the other PPSs will be analysed, using the process and methods previously described.

HESSD
7, 3551–3589, 2010

3.4.1 Set-up

Overlapping the physical core of the WRF-ARW model, the PPSs apply additional forcings to the model equations and fall into several categories given as options to the user. Above all possibilities, the microphysics, land surface and cumulus schemes probably have a major influence on the rain- and snowfall prediction, for acting directly on the atmosphere moisture content (land surface model), on the water vapour, cloud, and precipitation processes (microphysics) and on the resolution of convective processes (cumulus). The several experiments that were run are summarized in Table 4. Descriptions of these PPSs can be found in referenced papers.

3.4.2 Results

All the tests were applied to the experiments, though only a selection of the most significant scores are presented in Table 5. For this short event, the usage of different PPSs does not dramatically influence the precipitation output and therefore the statistical scores.

The most significant differences in the comparison with TRMM are to observe on the RMSD and MB scores and on the 100 mm event detection. Both cumulus PPSs show the most influence on these results, effect that would even be higher when considering the larger domain in its totality (here, only the area covered by the medium domain is considered, as for Fig. 3). The vast majority of convective induced precipitation in WRF output is occurring overseas and in the south of the Himalayas, while the grid-scale precipitation is reported over the mountains and the plateau. However, the two cumulus PPSs still substantially influence the precipitation output over the TiP. The CU2 experiment considerably reduces the mean precipitation estimation over the study area and smoothes the extremes but overestimates the occurrences of weaker events (but we showed that TRMM may underestimate precipitation areas). The CU1 experiment generally over-estimates precipitation fields. The other experiments show minor differences with the control experiment.

HESSD
7, 3551–3589, 2010

A larger impact of microphysics was to expect on the snowfall simulation (the totality of the precipitation over Nam Co was non-convective, in the form of snow), but the results are consistent for all schemes and the CU experiments show again the most differences. The LS1 scores for the smaller domain are considerably different as the evolution of the HSS is similar to the medium domain (curve not shown here) and the maximum is reached for a realistic threshold of 6 mm. However, the score is lower than for the other experiments.

In the comparison with ground measurements, the control experiment appears to be the most effective. The MP2 experiment outperforms considerably and the MP1 experiment has the lower MB (this is mostly due to an underestimation of precipitation at the station Deqen).

3.4.3 Summary

The impact of the PPSs on the model output is significant, but not dramatic: the initial error is not changed, but only partly meliorated or worsened. The sensitivity to cumulus and microphysics schemes is more important than to the land-surface model, and the cumulus schemes have more impact on the simulation of precipitation at lower altitude where WRF simulated the most part of convective induced rainfall. Even so, the global impact of the cumulus PPSs is also to be seen on snowfall estimation over the TiP. The New Grell-Devenyi 3 cumulus scheme had the best performance in reducing extreme precipitation amounts on the larger scale in reference to TRMM, and the control and land-surface experiments showed to have the best stability (no extremes). The comparison also showed that no definitive statement on a parameterization can be made because of the equal repartition of bad and good scores. For this event the New Grell-Devenyi 3 cumulus scheme seems to reduce the simulation bias over the TiP: this is consistent with the results of Chin (2008) and Yang and Tung (2003) who studied the model orographic bias over the complex terrain of California and Taiwan. The WSM6 microphysics scheme also provided good results.

HESSD
7, 3551–3589, 2010

4 Discussion and conclusion

In this paper, the capacities of the WRF model in retrieving precipitation fields over the Tibetan Plateau during a single event where analyzed, by comparing the output of the model with remote sensing data and ground observations. The event chosen for this purpose is the tropical cyclone Rashmi, which reached the coast of Bangladesh on 27 October 2008 and brought heavy precipitations over the Himalayas and the TiP. Three main questions where addressed:

(1) What are the validation tools and data available to the community to assess the performance of the model, and are they consistent enough for this purpose? In this study, we proposed three datasets (TRMM, MODIS, NCDC) and several statistical methods to assess the model simulation. It was intended to consider each dataset (WRF included) on an equal level as the other ones. In the first place, we discussed the mesoscale features of the event looking at WRF30 and TRMM datasets, and then we used statistical scores to quantify their discrepancy. Both WRF and TRMM agree on the distribution of precipitation (good HSS for 10 mm events), and on the movement of the precipitation front (Figs. 2 and 6). However, amounts and positions of the precipitation maximums do not always match, and WRF usually predicts more rainfall over larger areas. Even so, the comparison with MODIS and later with ground observations showed that in some cases, WRF may be closer to the real features than TRMM. The comparison with NCDC actually showed, for this event, a slight but general improvement from the WRF model over TRMM. Yin et al. (2008) already analysed TRMM errors over the TiP, but only during the summer season to avoid problems related to snowfall. To arrive to this conclusion, one assumes that ground observations can be taken as absolute reference. Yet the number of available stations is scarce and rain-gauge measurements are still subject to discussion. The sensitivity of rain gauges to wind and to the size of rain particles is very high, error that even worsens with snowfall: the snow catch efficiency of the four most widely used gauges can vary greatly, for example from 20% up to 70% (Goodison et al., 1998). In spite of these imperfections,

HESSD
7, 3551–3589, 2010

ground-based measurements are often assumed to be the most reliable and are taken as reference in many important studies (e.g., Mass et al., 2002; Yang and Tung, 2003). The discrepancy observed between all datasets (WRF, TRMM, NCDC) when looking at stations records on a case by case basis underlined how difficult it is to restore real precipitation. The contingency matrices based analysis partially reduces the problem by focusing on the spatio-temporal repartition of occurrences of an event and not on the exact retrieval of rainfall values. For the study of precipitation, this implies an arbitrary selection of intervals where amounts can be classified in events: this makes sense for product inter-comparisons or extreme events statistics, but not allways for operational purposes. Sometimes, like for the evaluation of snow with MODIS, no other possibilities are left. The comparison method proposed here has the strong disadvantage of being available only in very specific configurations (heavy snowfall over a region that was not snow covered before), but gives a very powerful and precise validation tool. The good accordance of WRF with MODIS was to see on the plots and was underlined by good contingency based scores. The lack of accuracy in the very small scales, as observed with the ground measurements records, also appeared applying these scores on the snowfall over the small domain (Fig. 5). To realize the sensitivity study in Sect. 3.4, we proposed to apply a combination of the methods described earlier. This avoids to reduce the description of model performance under one unique score and should diminish the risk of making mistakes in the decision process when assessing a model simulation. On the other side, it also increases the process complexity.

(2) Is it possible, between the numerous physical and spatial configurations of the WRF model, to propose a set-up that would be most adapted to the TiP area? The complete model set-up represents a countless number of possible configurations, and in this study there was no intent to realize a review of the different parameterization possibilities. Based on what we defined as our standard set-up, we first focused on the impact of resolution on the model output. Increasing resolution, among other benefits, spatially reduces the distances between available grid points and improves the static (time-invariant) terrestrial data resolution (if available). WRF bias and RMS deviations

HESSD
7, 3551–3589, 2010

in comparison to NCDC where reduced when going from the 30 to the 10 km resolution, yet the differences are rather low from the 10 to the 2 km resolution (this can be explained by the use of the two-way nesting option, that reflects nested domain output on the parent computation steps). In our study, we saw no good reason to give preference to the 2 km output more than to the 10 km, but we also lacked of observational data to assess the difference more accurately. Mass et al. (2002) arrived to similar conclusions using MM5 with 36, 12 and 4 km grids on a much longer time period. Sato et al. (2008) studied the precipitation diurnal cycle over the TiP and suggested that finer resolution at less than 7 km is necessary to simulate realistic features. This illustrates the necessity to adapt model output interpretation methods on an individual case basis, especially over the TiP, where there is a lack of both accurate input meteorological data as well as verification tools. Neither point measurements nor coarse grids can catch properly the spatially varying precipitation patterns, especially in mountainous terrains. Evolved interpolation methods such as inverse distance Cressman method where suggested to interpolate gridded data-sets to point based measurements (Colle et al., 1999), but if this is realistic for a constant varying field such as temperature, it does not always correspond to the complex spatial repartition of rainfall. After investigating the impact of resolution, we tested in a second approach how the model reacted to a different physical parameterization scheme configuration. We made use of widely used and experienced schemes, and our changes in the model parameterization did not affect dramatically the WRF precipitation output. For this weeklong event, no clear statement could be made on a peculiar best performing scheme, even if some differences could be noticed. Two experiments (CO1 and CU2) seem more adapted and demonstrated a good stability on the different scores and a global positive effect over the other experiments. For a higher statistical relevance, the study should be conducted on longer time periods and under different weather conditions.

(3) Is the model able to simulate and retrieve realistic precipitation fields in this mountainous and sparsely observed region? Some benefits of the model over usual precipitation products are quite obvious: e.g. high resolution on time and space (that can

HESSD
7, 3551–3589, 2010

be adjusted at will), flexibility and reproducibility. The model is also able to distinguish snow from rain and provides many additional meteorological variables simultaneously. Accuracy of both ground based measurements and TRMM algorithm in retrieving snowpack is an issue, and mesoscale weather forecasting models can become a good alternative to fill these gaps. Within the scope that we defined, our study shows that WRF capabilities in retrieving precipitation are good and can contribute to operational set-ups in combination with other products. However, the model also showed weak points and a tendency to over-estimate precipitation (in comparison with both TRMM and NCDC). Some undesired numerical effects and, eventually, inadequate input data can affect the operational output of the model for some extreme events, probably by exaggerating some physical processes (lake induced air moisture, orographic induced precipitation...). For many cases, WRF performed better than TRMM and recognized snow from rain with accuracy.

The results that are presented in this paper are relevant for a peculiar case and for a specific geographical region. They underlined the complexity of the problem when trying to define a dataset in which we can refer to, and a set of validation tools that suits to areas with few observational data. Many other model configurations could have been proposed and tested, but the relatively small sensitivity to both grid points size and physical parameterization scheme suggests that further investigation should be done on the model response to different meteorological and static boundary input data, parameters that may partly account for current errors on the precipitation forecast. It would be interesting to run the proposed tests on longer time periods for a stronger statistical relevance, and add verification datasets. With the exception of the Nam Co Station records, all data and models used in this study are available free of charge to the community. This recent melioration in data accessibility represents a great improvement and if these changes are conducted further on, they will enable many possibilities for future cooperative research.

HESSD
7, 3551–3589, 2010

Acknowledgements. This project was funded by the German Research Foundation (DFG) Priority Programme 1372, "Tibetan Plateau: Formation – Climate – Ecosystems" under the code SCHE 750/4-1. The authors wish to thank the staff of the Nam Co Station operated by the ITP-CAS for providing the useful data used in this study and and the GSFC DAAC for providing the TRMM data. We also made use of the MODIS products: these data are distributed by the Land Processes Distributed Active Archive Center (LP DAAC), located at the US Geological Survey (USGS) Earth Resources Observation and Science (EROS) Center (lpdaac.usgs.gov). The WRF model runs where carried out on the computer facility of the Technical University of Berlin.

References

Appel, E. and Mosbrugger, V.: Tibetan Plateau: Formation – Climate – Ecosystems: TiP, Science Plan For A Priority Programme, Tech. rep., 2006. 3553

Box, J. E., Bromwich, D. H., Veenhuis, B. A., Bai, L.-S., Stroeve, J. C., Rogers, J. C., Steffen, K., Haran, T., and Wang, S.-H.: Greenland ice sheet surface mass balance variability (1988–2004) from calibrated polar MM5 output, J. Climate, 19, 2783–2800, 2006.

Caldwell, P., Chin, H.-N. S., Bader, D. C., and Bala, G.: Evaluation of a WRF dynamical downscaling simulation over California, Climatic Change, 95, 499–521, doi:10.1007/s10584-009-9583-5, 2009.

Chen, F. and Dudhia, J.: Coupling an advanced land surface-hydrology model with the Penn State-NCAR MM5 modeling system, Part I: model implementation and sensitivity, Mon. Weather Rev., 129, 569–585, 2001. 3578

Chen, J., Li, C., and He, G.: A diagnostic analysis of the impact of complex terrain in the eastern Tibetan plateau, China, on a severe storm, Arct. Antarct. Alp. Res., 39, 699–707, 2007. 3556

Chin, H.-N. S.: Dynamical Downscaling of GCM Simulations: Toward the Improvement of Forecast Bias over California, Tech. rep., 2008. 3557, 3569

Colle, B., Westrick, K., and Mass, C.: Evaluation of MM5 and Eta-10 precipitation forecasts over the Pacific northwest during the cool season, Weather Forecast., 14, 137–154, 1999. 3572

Dudhia, J.: Numerical study of convection observed during the winter monsoon experiment using a mesoscale two-dimensional model, J. Atmos. Sci., 46, 3077–3107, 1989. 3578

HESSD

7, 3551–3589, 2010

Frauenfeld, O. W., Zhang, T., and Serreze, M. C.: Climate change and variability using European Centre for Medium-Range Weather Forecasts reanalysis (ERA-40) temperatures on the Tibetan Plateau, J. Geophys. Res., 110, D02101, doi:10.1029/2004JD005230, 2005. 3553

Gao, X., Xu, Y., Zhao, Z., Pal, J. S., and Giorgi, F.: On the role of resolution and topography in the simulation of East Asia precipitation, Theor. Appl. Climatol., 86, 173–185, doi:10.1007/s00704-005-0214-4, 2006. 3554

Gao, Y., Tang, M., Luo, S., Shen, Z., and Li, C.: Some aspects of recent research on the qinghai-xizang plateau meteorology, B. Am. Meteorol. Soc., 62, 31–35, 1981. 3552

Goodison, B., Louie, P., and Yang, D.: WMO solid precipitation measurement intercomparison, 1998.

Grell, G. A. and Dévényi, D.: A generalized approach to parameterizing convection combining ensemble and data assimilation techniques, Geophys. Res. Lett., 29(14), 1693, doi:10.1029/2002GL015311, 2002. 3581

Haginoya, S., Fujii, H., Kuwagata, T., Xu, J., Ishigooka, Y., Kang, S., and Zhang, Y.: Air-Lake Interaction Features Found in Heat and Water Exchanges over Nam Co on the Tibetan Plateau, Sola, 5, 172–175, 2009. 3557

Hahn, D. and Manabe, S.: Role of mountains in south asian monsoon circulation, J. Atmos. Sci., 32, 1515–1541, 1975. 3552

Hall, D. K., Riggs, G. A., and Salomonson, V. V.: MODIS/Terra Snow Cover Daily L3 Global 500 m Grid V005, 22–29 October 2008, Boulder, Colorado USA: National Snow and Ice Data Center, Digital media., 2006. 3558

Huffman, G. J., Adler, R. F., Bolvin, D. T., Gu, G., Nelkin, E. J., Bowman, K. P., et al.: The TRMM multi-satellite precipitation analysis: Quasi-global, multi-year, combined sensor precipitation estimates at fine scale., J. Hydrometeorol., 2007. 3558

IMD: Cyclonic Storm, RASHMI: A preliminary Report, http://www.imd.gov.in/section/nhac/dynamic/cycRashmi.pdf, 2008. 3556

Janjic, Z. I.: Nonsingular Implementation of the Mellor-Yamada Level 2.5 Scheme in the NCEP Meso model, Tech. Rep. 437, 2002. 3578

Kain, J. and Fritsch, J.: A one-dimensional entraining detraining plume model and its application in convective parameterization, J. Atmos. Sci., 47, 2784–2802, 1990. 3578

Kang, S., Chen, F., Gao, T., Zhang, Y., Yang, W., Yu, W., and Yao, T.: Early onset of rainy season suppresses glacier melt: a case study on Zhadang glacier, Tibetan Plateau, J. Glaciol., 55,

HESSD

7, 3551–3589, 2010

755–758, 2009. 3553
Kehrwald, N. M., Thompson, L. G., Tandong, Y., Mosley-Thompson, E., Schotterer, U., Alfimov, V., Beer, J., Eikenberg, J., and Davis, M. E.: Mass loss on Himalayan glacier endangers water resources, Geophys. Res. Lett., 35, L22503, doi:10.1029/2008GL035556, 2008. 3553
Leung, L. and Qian, Y.: The sensitivity of precipitation and snowpack simulations to model resolution via nesting in regions of complex terrain, J. Hydrometeorol., 4, 1025–1043, 2003. 3554
Li, M., Ma, Y., Hu, Z., Ishikawa, H., and Oku, Y.: Snow distribution over the Namco lake area of the Tibetan Plateau, Hydrol. Earth Syst. Sci., 13, 2023–2030, doi:10.5194/hess-13-2023-2009, 2009. 3554, 3557
Liu, J., Wang, S., Yu, S., Yang, D., and Zhang, L.: Climate warming and growth of high-elevation inland lakes on the Tibetan Plateau, Global Planet. Change, 67, 209–217, doi:10.1016/j.gloplacha.2009.03.010, 2009. 3553
Ma, L., Zhang, T., Frauenfeld, O. W., Ye, B., Yang, D., and Qin, D.: Evaluation of precipitation from the ERA-40, NCEP-1, and NCEP-2 Reanalyses and CMAP-1, CMAP-2, and GPCP-2 with ground-based measurements in China, J. Geophys. Res., 114, D09105, doi:10.1029/2008JD011178, 2009. 3553
Mass, C., Ovens, D., Westrick, K., and Colle, B.: Does increasing horizontal resolution produce more skillful forecasts? The results of two years of real-time numerical weather prediction over the Pacific northwest, B. Am. Meterol. Soc., 83, 407–430, 2002. 3554, 3571, 3572
Mlawer, E., Taubman, S., Brown, P., Iacono, M., and Clough, S.: Radiative transfer for inhomogeneous atmospheres: RRTM, a validated correlated-k model for the longwave, J. Geophys. Res.-Atmos., 102, 16663–16682, 1997. 3578
Peng, S., Xu, X., Shi, X., Wang, D., Zhu, Y., and Pu, J.: The early-warning effects of assimilation of the observations over the large-scale slope of the "World Roof" on its downstream weather forecasting, Chinese Sci. Bull., 54(4), 706–710, 2009. 3554
Rakesh, V., Singh, R., Pal, P. K., and Joshi, P. C.: Sensitivity of mesoscale model forecast during a satellite launch to different cumulus parameterization schemes in MM5, Pure Appl. Geophys., 164, 1617–1637, doi:10.1007/s00024-007-0245-0, 2007. 3555, 3563
Sato, T., Yoshikane, T., Satoh, M., Miltra, H., and Fujinami, H.: Resolution Dependency of the Diurnal Cycle of Convective Clouds over the Tibetan Plateau in a Mesoscale Model, J. Meteorol. Soc. Jpn., 86, 17–31, 2008. 3554, 3572
Shi, Y. and Liu, S.: Estimation on the response of glaciers in China to the global warming in the

HESSD
7, 3551–3589, 2010

21st century, Chinese Sci. Bull., 45, 668–672, 2000. 3556
Skamarock, W. C., Klemp, J. B., Dudhia, J., Gill, D. O., Barker, D. M., Duda, M. G., Huang, X.-Y., Wang, W., and Powers, J. G.: A Description of the Advanced Research WRF Version 3, Tech. rep., 2008. 3557
Smirnova, T., Brown, J., Benjamin, S., and Kim, D.: Parameterization of cold-season processes in the MAPS land-surface scheme, J. Geophys. Res.-Atmos., 105, 4077–4086, 2000. 3581
Tang, J., Zhao, M., and Su, B.: The effects of model resolution on the simulation of regional climate extreme events, Acta. Meteorol. Sin., 21, 129–140, 2007. 3554
Tao, W., Simpson, J., Baker, D., Braun, S., Chou, M., Ferrier, B., Johnson, D., Khain, A., Lang, S., Lynn, B., Shie, C., Starr, D., Sui, C., Wang, Y., and Wetzel, P.: Microphysics, radiation and surface processes in the Goddard Cumulus Ensemble (GCE) model, Meteorol. Atmos. Phys., 82, 97–137, doi:10.1007/s00703-001-0594-7, 2003. 3581
Thompson, G., Field, P. R., Rasmussen, R. M., and Hall, W. D.: Explicit Forecasts of Winter Precipitation Using an Improved Bulk Microphysics Scheme. Part II: implementation of a New Snow Parameterization, Mon. Weather Rev., 136, 5095–5115, doi:10.1175/2008MWR2387.1, 2008. 3578
Wilks, D. S.: Statistical Methods in the Atmospheric Sciences – An Introduction, vol. 59 of *International Geophysics Series*, Academic Press, 1995. 3559
Wu, T. and Qian, Z.: The relation between the Tibetan winter snow and the Asian summer monsoon and rainfall: an observational investigation, J. Climate, 16, 2038–2051, 2003. 3553
Wu, Y. and Zhu, L.: The response of lake-glacier variations to climate change in Nam Co Catchment, central Tibetan Plateau, during 1970–2000, J. Geogr. Sci., 18, 177–189, doi:10.1007/s11442-008-0177-3, 2008. 3553
Yang, M. and Tung, Q.: Evaluation of rainfall forecasts over Taiwan by four cumulus parameterization schemes, J. Meteorol. Soc. Jpn., 81, 1163–1183, 2003. 3555, 3569, 3571
Yao, T., Pu, J., Lu, A., Wang, Y., and Yu, W.: Recent glacial retreat and its impact on hydrological processes on the tibetan plateau, China, and sorrounding regions, Arct. Antarct. Alp. Res., 39, 642–650, 2007. 3553
Yin, Z.-Y., Zhang, X., Liu, X., Colella, M., and Chen, X.: An assessment of the biases of satellite rainfall estimates over the Tibetan Plateau and correction methods based on topographic analysis, J. Hydrometeorol., 9, 301–326, doi:10.1175/2007JHM903.1, 2008. 3553, 3570
Zhu, G. and Chen, S.: A numerical case study on a mesoscale convective system over the Qinghai-Xizang (Tibetan) Plateau, Adv. Atmos. Sci., 20, 385–397, 2003. 3554

HESSD
7, 3551–3589, 2010

Table 1. WRF model set-up.

Physical parametrization of the control experiment	
Microphysics	Modified Thompson scheme (Thompson et al., 2008)
Boundary layer parameterization	Mellor-Yamada-Janjic TKE scheme (Janjic, 2002)
Cumulus parameterization	Kain-Fritsch (Kain and Fritsch, 1990) scheme (exept for 2 km domain: no cumulus)
Land-surface model	Noah Land-surface Model (LSM) (Chen and Dudhia, 2001)
Longwave radiation	Rapid Radiative Transfer Model (RRTM) (Mlawer et al., 1997)
Shortwave radiation	Dudhia scheme (Dudhia, 1989)
Driving data	
Surface and lateral boundary	NCEP/FNL from GFS Operational Model Global Tropospheric Analyses (1°, 6 hourly)
Sea surface temperature	NCEP/MMAB real-time, global, sea surface temperature (RTG_SST) analysis (0.5°, daily)
Map and grids	
Map projection	Lambert conformal
Center point of domain	28.85° N , 89.57° E
Number of vertical layers	28
Nesting	1 parent, 2 nested domains, Two-way nesting option
Horizontal grid spacing	30 km, 10 km, 2 km
Unstaggered grid points	150×150, 150×150, 150×150
Runge-Kutta (RK3) time step	120 s, 40 s, 8 s
Static geographical fields	USGS standard dataset at 10 m, 5 m, 30′ resolution
Simulation time	
Starting time	Daily, 12:00 UTC
Simulation duration	36 h
Spin up	12 h

HESSD
7, 3551–3589, 2010

Table 2. Contingency table used for verification. Each element of the matrix holds the number of occurrences in which the observations and/or the model observed a given event.

		Observed	
	Event	Yes	No
WRF	Yes	A	B
	No	C	D

HESSD
7, 3551–3589, 2010

Table 3. Accumulated precipitation (mm/7 days) for each station from NCDC, TRMM, WRF30, WRF10 and WRF2. The Nam Co station (N20) is not part of the NCDC dataset. Root Mean Square Error (RMSE) and Mean Bias (MB) are given for comparison. The time-series of stations marked with a (*) are presented on Fig. 6.

Id	Station	Lon	Lat	Alt. (m)	NCDC	TRMM	WRF30	WRF10	WRF2
01*	BAINGOIN	90.02	31.37	4701	06.1	08.2	09.1	07.0	07.9
02	DEGE	98.57	31.80	3185	12.2	24.6	44.2	40.4	
03	DENGQEN	95.60	31.42	3874	36.6	22.6	51.5	46.2	
04*	DEQEN	98.88	28.45	3320	138.4	26.7	212.3	147.7	
05*	LHASA	91.13	29.67	3650	06.9	47.8	43.0	36.9	34.3
06*	LHUNZE	92.47	28.42	3861	25.1	55.5	36.3	29.3	
07	MADOI	98.22	34.92	4273	06.1	04.9	05.5	04.5	
08	NAGQU	92.07	31.48	4508	22.1	23.0	24.2	22.2	21.8
09*	NYINGCHI	94.47	29.57	3001	46.2	30.4	78.9	58.1	
10*	PAGRI	89.08	27.73	4300	65.0	69.7	45.0	46.6	
11	QAMDO	97.17	31.15	3307	25.9	17.3	38.7	38.8	
12	QUMARLEB	95.78	34.13	4176	11.9	04.6	20.6	18.5	
13*	SOG XIAN	93.78	31.88	4024	30.2	75.7	42.9	37.7	
14	TINGRI	87.08	28.63	4300	00.0	28.1	00.0	00.0	
15	TUOTUOHE	92.43	34.22	4535	00.8	01.4	04.9	05.3	
16	XAINZA	88.63	30.95	4670	02.0	29.9	01.0	00.8	
17	XIGAZE	88.88	29.25	3837	05.8	19.8	14.8	08.3	
18*	YUSHU	97.02	33.02	3682	26.9	03.1	39.6	38.0	
19	ZADOI	95.30	32.90	4068	17.3	29.3	41.6	43.2	
20*	NAMCO	90.98	30.77	4730	15.9	18.9	26.4	31.8	31.0
				Total	495.3	533.3	771.4	654.3	
				RMSD		31.9	23.4	13.6	
				MB		02.0	13.9	08.0	

HESSD
7, 3551–3589, 2010

Table 4. Physical parameterization set-ups.

Name	Experiment	New parametrization
CU1	Cumulus	Betts-Miller-Janjic (BMJ) scheme
CU2	Cumulus	New Grell-Devenyi 3 sheme (Grell and Devenyi, 2002)
MP1	Microphysics	WRF Single-Moment 6-class (WSM6) scheme
MP2	Microphysics	Goddard Cumulus Ensemble (GCE) models (Tao et al., 2003)
LS1	Land cover	Rapid Update Cycle (RUC) Model (Smirnova et al., 2000)

HESSD
7, 3551–3589, 2010

Table 5. Statistical evaluation scores for the control and the five sensitivity experiments. Best performing experiments are marked with a *, worst performing with a °. In addition to the WRF/MODIS scores, the threshold for which the best HSS is obtained is indicated.

Scores/Experiment	CO1	CU1	CU2	LS1	MP1	MP2
WRF30/TRMM, T=10 mm, BIAS	1.075	1.082	1.127°	1.082	1.049*	1.058
WRF30/TRMM, T=10 mm, HSS	0.678	0.680	0.649°	0.687	0.696	0.697*
WRF30/TRMM, T=100 mm, BIAS	8.246	9.018°	7.140*	8.175	8.070	8.298
WRF30/TRMM, T=100 mm, HSS	0.151	0.136°	0.160*	0.153	0.147	0.150
WRF30/TRMM, RMSD	62.93	70.63°	51.98*	63.40	63.85	61.76
WRF30/TRMM, MB	26.75	31.15°	21.57*	27.69	25.82	27.01
WRF10/MODIS, HSS Max	0.700°	0.732*	0.712	0.708	0.708	0.704
Threshold (mm/7days)	7	6	8	8	6	6
WRF2/MODIS, HSS Max	0.427	0.418	0.433*	0.339°	0.412	0.411
Threshold (mm/7days)	2	2	2	6	2	3
WRF10/NCDC, RMSE	13.64*	14.08	14.21	13.78	14.96	20.09°
WRF10/NCDC, MB	7.98	5.97	6.74	9.56	2.01*	12.33°

HESSD
7, 3551–3589, 2010

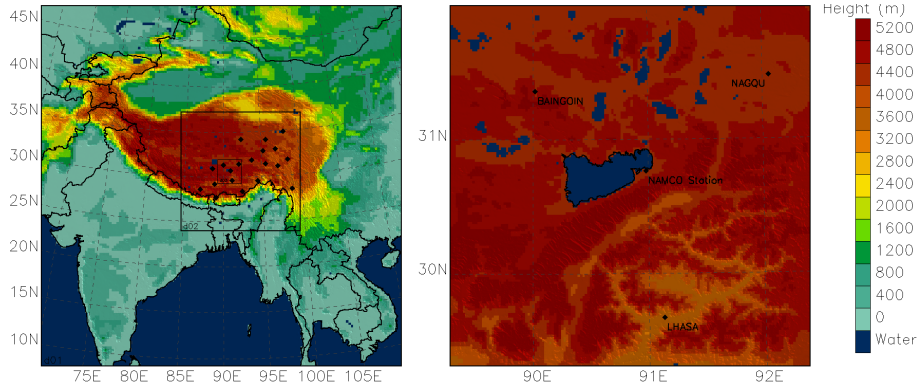

Fig. 1. Left: WRF domain definitions: large (30 km grid size), medium (10 km) and small (2 km) centred on the Nam Co Basin. Right: The smaller domain and Nam Co lakeshore. The black dots represent the positions of the available meteorological stations.

HESSD
7, 3551–3589, 2010

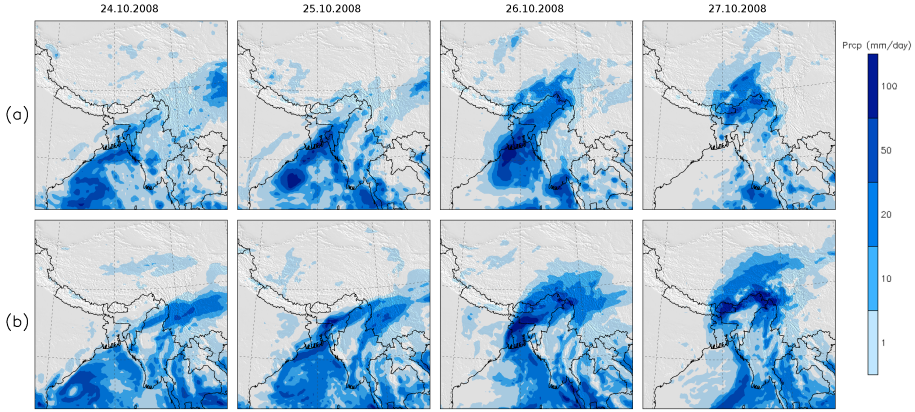

Fig. 2. Daily accumulated precipitation fields from **(a)** TRMM and **(b)** WRF30 over the bay of Bengal and the Tibetan Plateau for the period 24–27 October 2008.

HESSD
7, 3551–3589, 2010

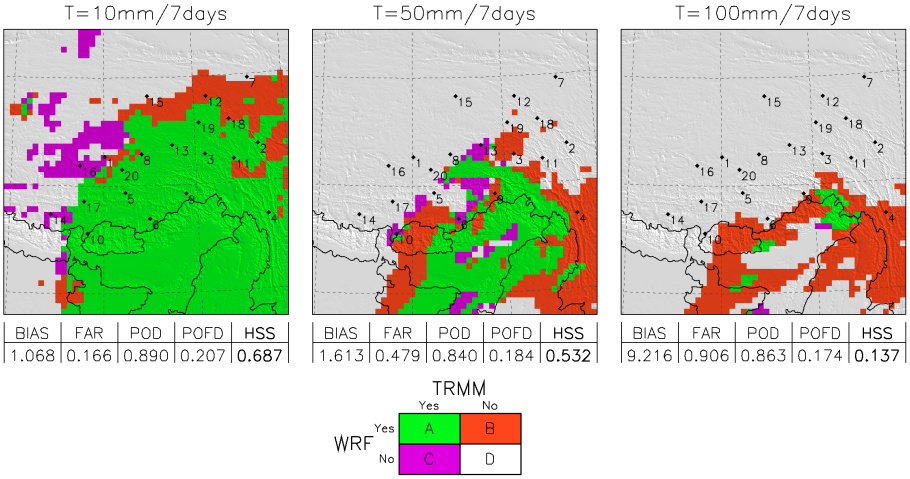

Fig. 3. Seven days accumulated precipitation fields from TRMM and WRF30, each grid point is classified following the contingency table conventions for the 10, 50 and 100 mm events. The corresponding scores are given under each plot, and meteorological stations positions are indicated.

HESSD
7, 3551–3589, 2010

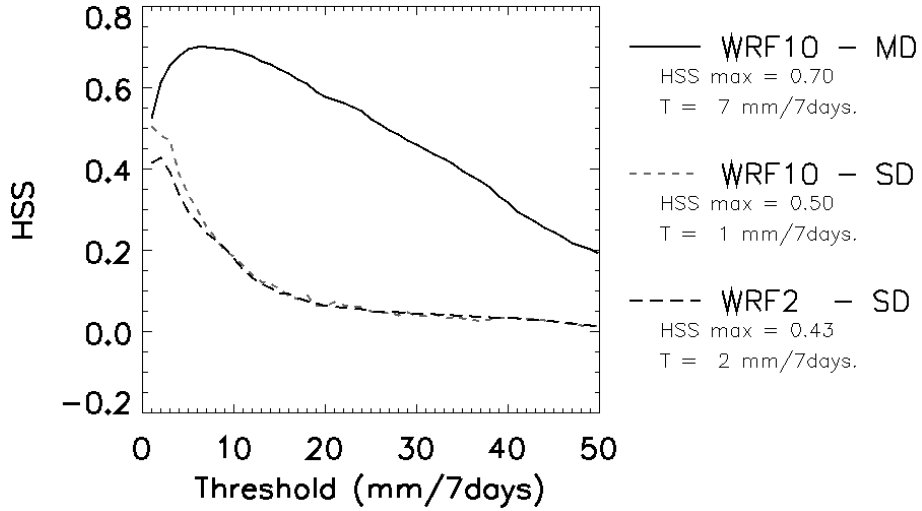

Fig. 4. WRF snowfall fields in comparison with MODIS. Evolution of the HSS score with the augmentation of the threshold applied to the seven days accumulated snowfall from: (1) WRF10 output over the medium domain (MD), (2) WRF10 output over the small domain (SD) and (3) WRF2 output over the small domain. The best scores and corresponding optimal thresholds are given for information.

HESSD
7, 3551–3589, 2010

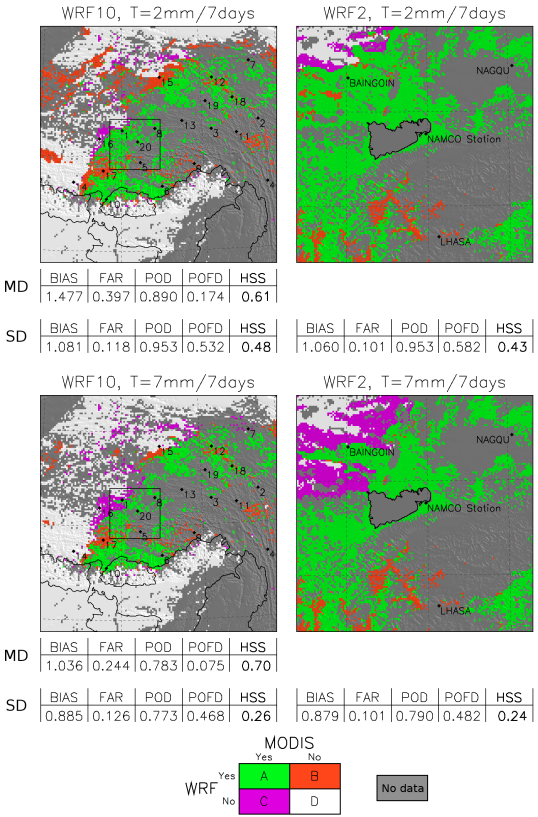

Fig. 5. Seven days accumulated snowfall fields that reached the thresholds 2 and 7 mm/7 days for WRF10 and WRF2 datasets in comparison with MODIS. Each grid point is classified following the contingency table conventions. The corresponding scores for are given under each plot, for the medium domain (MD) and the small domain (SD), and meteorological stations positions are indicated.

HESSD
7, 3551–3589, 2010

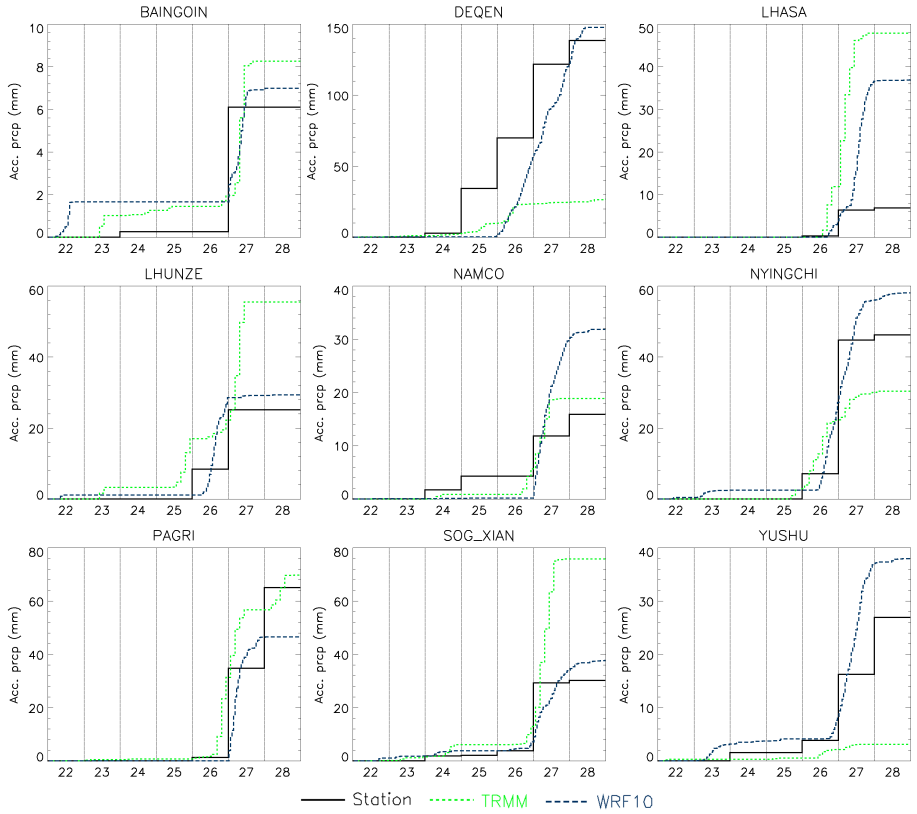

Fig. 6. Accumulated precipitation time-series (Acc. prcp, in mm) from NCDC, TRMM and WRF10 for a selection of nine meteorological stations. Units on the x-axis are the days in October 2008. Data time resolution is respectively: daily, 3-hourly, and hourly.

HESSD
7, 3551–3589, 2010

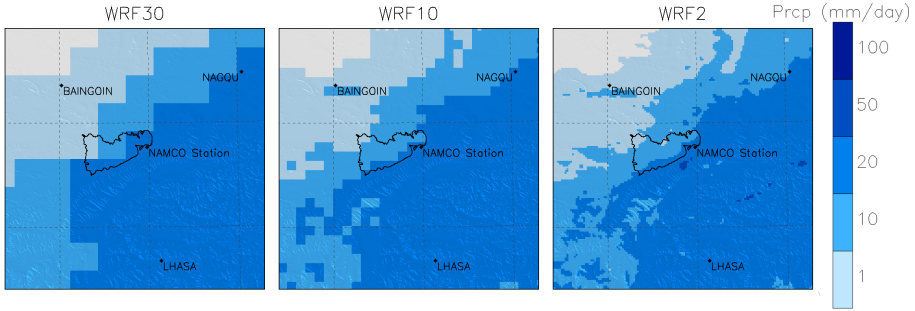

Fig. 7. Precipitation fields from WRF30, WRF10 and WRF2 over the Nam Co Basin on the 27 October 2008.

HESSD
7, 3551–3589, 2010